

Article

Photorefractive Properties of Molybdenum and Hafnium Co-Doped LiNbO₃ Crystals

Ling Zhu ¹ , Dahuai Zheng ^{2,*} , Shahzad Saeed ¹ , Shuolin Wang ¹, Hongde Liu ¹,
Yongfa Kong ^{1,2,*}, Shiguo Liu ¹, Shaolin Chen ², Ling Zhang ² and Jingjun Xu ^{1,2}

¹ School of Physics, Nankai University, Tianjin 300071, China; 1120110056@mail.nankai.edu.cn (L.Z.); shehzadsaeed2003@yahoo.com (S.S.); 2120170156@mail.nankai.edu.cn (S.W.); liuhd97@nankai.edu.cn (H.L.); nkliusg@nankai.edu.cn (S.L.); jjxu@nankai.edu.cn (J.X.)

² The MOE Key Laboratory of Weak-Light Nonlinear Photonics and TEDA Institute of Applied Physics, Nankai University, Tianjin 300457, China; chenshaolin@nankai.edu.cn (S.C.); zhangl63@nankai.edu.cn (L.Z.)

* Correspondence: dhzheng@nankai.edu.cn (D.Z.); kongyf@nankai.edu.cn (Y.K.);
Tel.: +86-138-2182-6517 (D.Z.); +86-138-0219-3619 (Y.K.)

Received: 10 July 2018; Accepted: 10 August 2018; Published: 13 August 2018



Abstract: A series of LiNbO₃: Mo, Hf crystals with 0.5 mol % fixed MoO₃ and various HfO₂ concentrations (0.0, 2.0, and 3.5 mol %) were grown by the Czochralski technique. The photorefractive properties of the LiNbO₃: Mo, Hf crystals were investigated by two-wave coupling measurements and the beam distortion method was employed to obtain the optical damage resistance ability. The UV-visible and OH⁻ absorption spectra were also studied. The experimental results imply that the photorefractive properties of LiNbO₃: Mo crystals at laser wavelengths of 532, 488, and 442 nm can be greatly enhanced by doping HfO₂ over the threshold concentration. At 442 nm especially, the response time of LN: Mo, Hf_{3.5} can be shortened to 0.9 s with a diffraction efficiency of 46.07% and a photorefractive sensitivity reaching 6.28 cm/J. Besides this, the optical damage resistance at 532 nm is 3 orders of magnitude higher than that of the mono-doped LiNbO₃: Mo crystal, which is beneficial for applying it in the field of high-intensity lasers.

Keywords: LiNbO₃ crystal; molybdenum and hafnium co-doping; photorefractive properties

1. Introduction

Lithium niobate (LiNbO₃, or LN) crystal is one of the most prominent materials for applications in many practical fields, such as optical modulators [1], holographic storage [2], waveguides [3,4], resonators [5], and integrated optics devices, resulting from its superior and diverse physical performance [6,7]. In recent decades, crystal growth, defect structures, photorefractive properties, phase-matching, and theoretical simulations have been studied in depth and substantial research progress has been reported for LN crystals [7–10]. Meanwhile, the control of photorefraction, i.e., saturated diffraction efficiency, response time, etc., is one of the most important research fields. The incorporation of transition metal ions, such as Fe, Cu, and Mn, can enhance the photorefractive properties of LN crystals [11–13], while Mg, In, Zr, and Hf ions would increase the optical damage resistance of LN crystals [14–16]. Recently, Tian et al. reported that hexavalent Mo⁶⁺ doping can tremendously enhance the photorefractive properties of LN crystals [17]. Nevertheless, similarly to mono-doped Fe ions, there are still many obstacles, including low optical damage resistance and insufficient response time, which restrict their use in commercial applications. We know that the double or triple co-doping of iron-doped lithium niobate crystals can improve these properties to some extent [18–20]. The subsequent work of Tian et al. draws the conclusion that when the concentration of bivalent Mg²⁺ exceeds the threshold, the response time of LN: Mo, Mg crystal can be greatly shortened

(0.22 s at 351 nm), but tetravalent Zr^{4+} drastically reduces the photorefractive properties of LN: Mo crystal [21]. Depending on whether the effect of the valence state of dopants on the properties of lithium niobate has a common character, it is necessary to add other tetravalent dopants into LN: Mo crystal to explore the inherent law. On the other hand, the doping threshold of tetravalent dopants, such as Hf^{4+} , Sn^{4+} , and Zr^{4+} , is low and the distribution coefficient is close to 1.0, which is favorable for the growth of high-quality crystals. However, based on our previous work experience, it is easier to grow Hf^{4+} -doped LN than Sn^{4+} -doped LN.

In this work, Hf^{4+} was selected as the co-doped dopant for LN: Mo crystal. Hf^{4+} and Mo^{6+} co-doped LN crystals with various Hf^{4+} doping levels were grown and their photorefractive properties and UV-visible and OH^- absorption spectra were investigated. Our goal was to ascertain the impact of Hf^{4+} on the photorefractive performance of LN: Mo crystal.

2. Materials and Methods

The conventional Czochralski method was applied to grow LN: Mo, Hf crystals [22]. On the basis of previous work, the optimal results were obtained when the doping concentration of Mo^{6+} was 0.5 mol %, and for Hf^{4+} the doping threshold is between 2.0 and 2.5 mol % [17,23]. Therefore, we fixed the concentration of Mo^{6+} at 0.5 mol % and selected the Hf^{4+} concentrations of 0.0, 2.0, and 3.5 mol %, which are labeled as LN: Mo, LN: Mo, $Hf_{2.0}$, and LN: Mo, $Hf_{3.5}$, respectively. The $[Li]/[Nb]$ ratio for all the samples was 48.38/51.62. A congruent LN crystal was also grown for comparison and named CLN. The as-grown crystals were polarized in air at 1150 °C; the polarization current was 30 mA and the duration time was 15 minutes. Finally, we cut 3.0-mm-thick and 1.0-mm-thick y-oriented samples from the crystals and polished them to optical grade.

We used the 3-mm-thick y-oriented plates to study the photorefractive properties of LN: Mo, Hf crystals by the two-wave coupling method. The laser wavelengths we selected for the measurements were 442, 488, and 532 nm from a (continuous wave) CW frequency-doubled solid-state laser, an Ar^+ laser, and a He-Cd laser, respectively. An optical splitter was employed to split the extraordinary polarized laser into two equal-intensity beams (400 mW/cm² each), which were then reflected by mirrors and incident on the crystals at an appropriate crossing angle. In order to utilize the maximum electro-optic coefficient γ_{33} , the grating vector should be kept along the c axis of the crystal. The intensity of the diffracted light I_d and transmitted light I_t was measured directly by the detectors after passing through the crystal. We defined the diffraction efficiency as $\eta = I_d/(I_d + I_t)$ and then fitted the curve of “ η ” versus time “ t ” by the function $\eta_t = \eta_s (1 - e^{-t/\tau_r})^2$ to get the saturated diffraction efficiency η_s and the response time τ_r . Further, the photorefractive sensitivity is defined as $S = (\partial\sqrt{\eta}/\partial t)_t = 0/I_d$. Here, “ I ” is the recording light intensity and “ d ” is the thickness of the samples.

The optical damage resistance ability of all samples was investigated by the beam distortion method and a sample size of 3-mm-thick y-oriented plates. When the laser is focused on the crystal, the transmitted beam will become distorted once the laser intensity exceeds a certain value: we consider this intensity as the optical damage threshold of the crystals. We obtained the optical damage threshold for the crystals by directly observing the shape of the transmitted beam spot. The 532 nm wavelength laser (the CNI MGL-III-532 laser, Changchun New Industries Optoelectronics Tech. Co., Ltd., Changchun, China) was selected for this experiment; also, we used a 30-mm lens for focusing the beam into the crystal to obtain a higher light intensity.

The UV-visible absorption spectra were measured by a UV-4100 spectrophotometer (Hitachi Science and Technology, Tokyo, Japan) with a range of 300–800 nm and resolution of 1 nm. A MAGNA-560 FT-IR spectrometer (Thermo Nicolet Corporation, Madison, America) was used for infrared (IR) spectroscopy with a test range of 400–4000 cm⁻¹ and a resolution of 2 cm⁻¹. Both of the samples were 1-mm y-oriented plates for the spectrum measurements and the incoming light was unpolarized.

3. Results

3.1. Two-Wave Coupling Measurements

Figure 1 shows the photorefractive properties of LN: Mo, Hf crystals at the 442, 488, and 532 nm laser wavelengths. The saturated diffraction deficiency (η_s) is described in Figure 1a, the response time in Figure 1b, and the sensitivity in Figure 1c. We can see from Figure 1a that, compared with CLN, the saturated diffraction efficiency of all LN: Mo, Hf crystals is improved. The η_s of each sample measured at 442 nm is higher than that at 488 nm and 532 nm. The η_s of LN: Mo, Hf_{3.5} crystal can reach 46.07% at the 442 nm laser wavelength, which is about 10 percent higher than that of LN: Mo crystal. However, the η_s slightly decreased for LN: Mo, Hf_{2.0} with respect to LN: Mo at all three wavelengths and for LN: Mo, Hf_{3.5} at 488 and 532 nm. As shown in Figure 1b, the response time of all LN: Mo, Hf crystals has been greatly shortened compared with that of CLN crystal. For LN: Mo, Hf_{2.0}, there is no amendment in the response speed compared to LN: Mo crystal. However, for LN: Mo, Hf_{3.5} crystal, when the concentration of Hf exceeds the threshold, we can obtain the minimum response times of 1.93 s, 2.06 s, and 0.9 s at 532 nm, 488 nm, and 442 nm, respectively, which are several times lower than that of LN: Mo crystal. Moreover, Figure 1c indicates that the sensitivity for all samples is greatly enhanced at 442 nm and slightly different in value at 488 nm and 532 nm, respectively. For LN: Mo, Hf_{3.5}, we obtain the highest sensitivity of 6.28 cm/J at 442 nm.

The above experimental results indicate that the incorporation of Hf⁴⁺ above the threshold can greatly enhance the photorefractive properties of LN: Mo crystal.

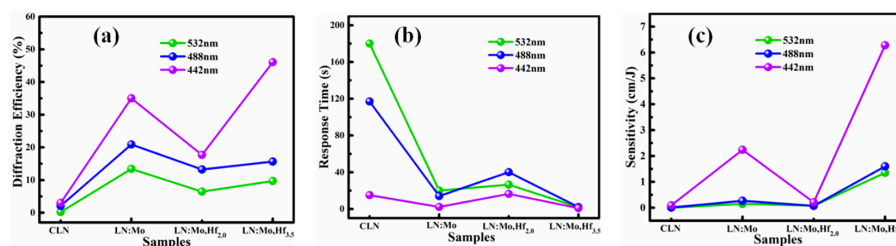


Figure 1. Photorefractive properties of Lithium niobate (LN): Mo crystals co-doped with different concentrations of Hf with a light intensity of 400 mW/cm² per beam at laser wavelengths of 532, 488, and 442 nm. Control LN (CLN) crystal is also presented for comparison. (a) Diffraction efficiency; (b) Response time; and (c) Sensitivity.

3.2. Optical Damage Resistance

Figure 2 shows the transmitted light beam distortion of LN: Mo, Hf samples, which were irradiated by a 532-nm wavelength laser for 5 min. CLN crystal is also listed for comparison. As shown in Figure 2d, the optical damage threshold for LN: Mo, Hf_{3.5} crystal was found to be about 1.54×10^4 W/cm²; which is 3 orders of magnitude higher than optical damage threshold for mono-doped Mo⁶⁺ crystals (Figure 2b, the transmitted light beam was blurred at the very low intensity of 5.93×10 W/cm²). LN: Mo, Hf_{2.0} crystal is unable to withstand a laser power density of 1.54×10^4 W/cm² (Figure 2c).

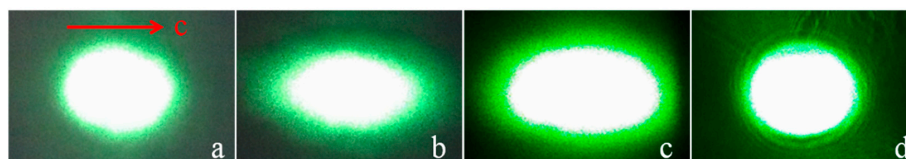


Figure 2. Transmitted laser beam spots of an incident 532-nm wavelength laser after 5 min of irradiation: (a) CLN; (b) LN: Mo; (c) LN: Mo, Hf_{2.0}; (d) LN: Mo, Hf_{3.5}. The light intensity was 59.3 W/cm² for (a,b) and 1.54×10^4 W/cm² for (c,d).

The LN: Mo crystal has good photorefractive properties, but it exhibits optical damage at a very low light intensity. Obviously, it is not conducive to commercial applications of high laser intensities. The above results suggest that Hf incorporation is an effective way to enhance the optical damage resistance of LN: Mo crystal, and can also advance its application in the field of high-intensity lasers.

3.3. UV-Visible Absorption Spectra

We employed a UV-4100 spectrophotometer to measure the UV-visible absorption spectra. Figure 3 shows the results of the UV-Vis absorption spectra for LN: Mo, Hf crystals with different Hf⁴⁺ doping levels along with those of CLN crystal for comparison. The inset figure shows the absorption spectra near the absorption band edge. Compared with CLN crystal, there are noticeable red-shifts for LN: Mo crystals. With an increase in Hf⁴⁺ doping concentration, violet-shifts occur for LN: Mo, Hf crystals compared to LN, Mo crystal.

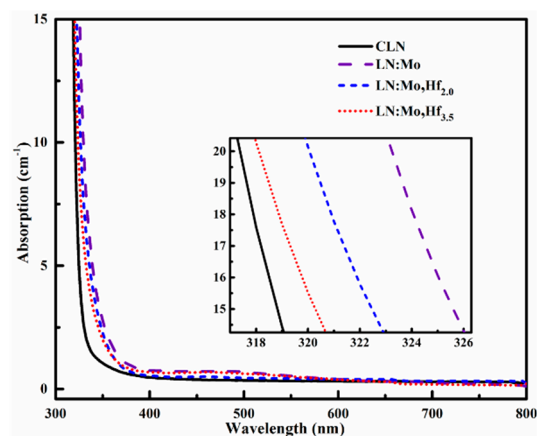


Figure 3. Absorption spectra of LN: Mo, Hf and congruent LN crystals, while the inset is the absorption spectra near the absorption edge.

Based on the accumulated results, Mo⁶⁺ in the LN crystal structure preferentially occupies the Nb sites and pushes regular Nb⁵⁺ to Li sites, forming new defects of Mo_{Nb}⁺ [17]. A large number of anti-site Nb_{Li}⁴⁺ cause a significant red-shift in the absorption edge of LN: Mo crystals. With the doping of Hf⁴⁺ in LN: Mo crystal, Nb_{Li}⁴⁺ will be mostly substituted by Hf⁴⁺; thus, a violet-shift of the absorption edge occurs in LN: Mo, Hf_{3.5} crystal.

3.4. OH⁻ Absorption Spectra

The infrared (IR) spectroscopy of samples was measured within the test range of 400–4000 cm⁻¹ and the resolution of 2 cm⁻¹. It is well-known that there is a threshold concentration for optical-damage-resistant dopants in LN crystals, which would result in analogous characteristic movements of the OH⁻ absorption peak [24]. The OH⁻ absorption peak of the CLN crystal is about 3484 cm⁻¹, so for comparison we only took values between 3420 cm⁻¹ and 3560 cm⁻¹ and then normalized them. Based on previous reports, the shift of Hf-doped LiNbO₃ crystals is very slight [23], and it is necessary to study the internal structure of the OH⁻ absorption peak in more detail. The OH⁻ absorption band of CLN crystal is broad, and we can decompose it into three peaks, in which the peak of 3466 cm⁻¹ is thought to be caused by the direct substitution of protons for Li⁺ ions, while the 3481 and 3489 cm⁻¹ peaks are due to protons occupying the Li vacancy (V_{Li}⁻) in two different ion environments near Nb_{Li}⁴⁺ [25]. Moreover, according to the shape of the Hf-doped LiNbO₃ difference spectra, it is conceivable that the absorption peak can also be decomposed into three peaks [26,27].

The OH⁻ absorption spectra of LN: Mo, Hf and CLN crystals are shown in Figure 4. Just as expected, there is only a slight shift of the OH⁻ vibration absorption band for both LN: Mo, Hf_{2.0} and LN: Mo, Hf_{3.5} crystals. Therefore, the three-decomposed-peaks model was employed. We separately

decomposed the absorption bands of LN: Mo, Hf crystals into three peaks by Lorentz fitting. We tried to fit the peak of 3466 or 3475 cm^{-1} [28] for both LN: Mo, Hf_{2.0} and LN: Mo, Hf_{3.5} crystals, but the fit was not good; only when the peaks were located at 3481, 3490, and 3500 cm^{-1} could we obtain good fittings. We can see in Figure 5a that for LN: Mo, Hf_{2.0}, the peak at 3490 cm^{-1} is the highest. As shown in Figure 5b, the three fitted peaks of LN: Mo, Hf_{3.5} crystal are also located at 3481, 3490, and 3500 cm^{-1} , but the highest peak is at 3481 cm^{-1} and the lowest one is at 3500 cm^{-1} . It is necessary to further discuss the influence of ion locations on the OH⁻ stretching vibration spectra.

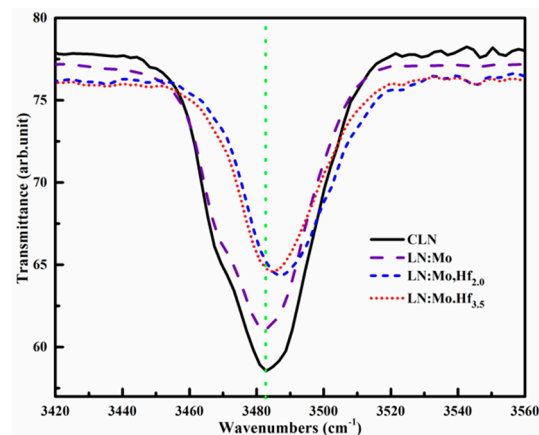


Figure 4. The OH⁻ spectra of LN: Mo, Hf crystals with different concentrations of Hf⁴⁺. The spectrum of CLN is presented for comparison.

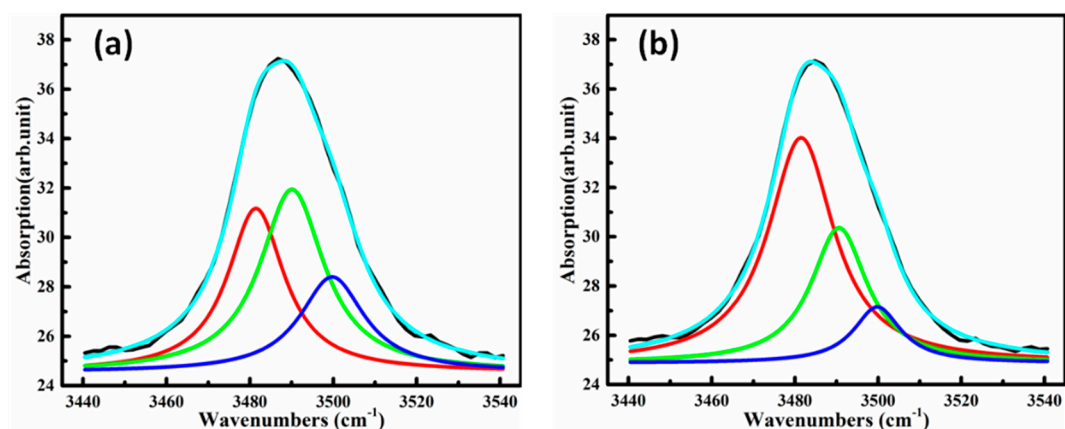


Figure 5. The components of OH⁻ absorption spectra of LN: Mo, Hf crystals. (a) LN: Mo, Hf_{2.0}; (b) LN: Mo, Hf_{3.5}.

4. Discussion

According to previous reports, in mono-Hf-doped CLN crystals, due to the strong electronegativity of Hf_{Li}³⁺, the components near 3484 cm^{-1} are formed by H⁺ occupying V_{Li}⁻ around not only Nb_{Li}⁴⁺ ions but also Hf_{Li}³⁺ ions, and the H⁺'s direct compensation for the negatively charged Hf_{Nb}⁻ should be the reason for the component of 3500 cm^{-1} [25]. Besides this, the OH⁻ vibrational frequency is found at 3475 cm^{-1} in Hf-doped stoichiometric LN crystals, which represents the Hf_{Nb}⁻-OH defect [28]. What is more, there are Mo⁴⁺, Mo⁵⁺, and Mo⁶⁺ ions in our samples [17]. All these complex factors make it difficult for us to deduce the specific substitution sites in our samples. Compared with previous results [25,28], the difference may be caused by the complicated valence of Mo ions in LN: Mo, Hf crystals; consequently, this needs further investigation.

As reported, Zr^{4+} cannot improve the response speed of LN: Mo crystals even when its doping concentration exceeds the threshold. When the concentration of Mg^{2+} exceeds the threshold, very short photorefractive response times of 0.22 s, 0.33 s, 0.37 s, and 1.2 s for 351, 488, 532, and 671 nm, respectively, were obtained [21]. From the present results, when the Hf^{4+} concentration exceeds the threshold, it can greatly enhance the photorefractive properties of LN: Mo crystal, though the effects are still slightly weaker as compared with those of Mg^{2+} . Firstly, we believe that the defects related to Mo ions (Mo^{4+} , Mo^{5+} , and Mo^{6+}) play the main role of photorefractive centers in our samples. Compared with Mg^{2+} , when the doping concentration of Zr^{4+} and Hf^{4+} reaches the threshold, Zr_{Li}^{3+} and Hf_{Li}^{3+} could not completely replace the Mo_{Li}^{3+} resulting from Zr^{4+} , as Hf^{4+} and Mo^{4+} have the same valence. This would lead to a lower concentration of Mo_{Nb}^{+} in LN: Mo, Zr and LN: Mo, Hf crystals. In addition, $Zr_{Nb}^{-}-Mo_{Nb}^{+}$ and $Hf_{Nb}^{-}-Mo_{Nb}^{+}$ will form more stable defect clusters than $Mg_{Nb}^{3-}-3Mo_{Nb}^{+}$, which actually weaken the role of Mo_{Nb}^{+} as a photorefractive center in LN: Mo, Zr and LN: Mo, Hf crystals. Therefore, the photorefractive properties of both samples cannot be significantly enhanced compared with LN: Mo, Mg crystals. Secondly, as for Zr^{4+} and Hf^{4+} , Hf^{4+} has the same valence as Zr^{4+} . Checking the periodic table of elements, we can find that Zr and Nb are adjacent elements in the same cycle while Hf is in the next cycle. This shows that Nb and Zr have more similar properties; hence, Zr^{4+} would be more likely to occupy Nb sites than Hf^{4+} , and it is easier for Hf^{4+} to replace Mo ions at the Li sites than it is for Zr^{4+} . Consequently, the amount of Mo_{Nb}^{+} in LN: Mo, Hf crystals will be greater than that in LN: Mo, Zr crystals; then, LN: Mo, Hf crystals will have better photorefractive properties than LN: Mo, Zr crystals. Finally, these assumptions need further investigation.

5. Conclusions

Lithium niobate crystals co-doped with molybdenum and hafnium were grown and their photorefractive properties were studied with 532, 488, and 442 nm wavelength lasers. The results clearly describe that, different from the incorporation of Zr^{4+} , which drastically reduces the photorefractive properties of LN: Mo crystal, Hf^{4+} co-doping can greatly enhance the photorefractive properties of LN: Mo crystal when the Hf^{4+} doping concentration is over the threshold. The doping of hafnium over the threshold is an effective method to improve the photorefractive properties of LN: Mo crystals. In detail, the optical damage resistance of LN: Mo, $Hf_{3.5}$ crystal was 3 orders of magnitude higher than that of mono-doped Mo: $LiNbO_3$ crystal at the 532 nm laser wavelength. The response time of LN: Mo, $Hf_{3.5}$ crystal can be shortened to 0.9 s with a diffraction efficiency of 46.07%, and the photorefractive sensitivity can reach 6.28 cm/J at the 442 nm laser wavelength. These results can play a good role in further tuning the performance of LN crystals and promoting their practical application.

Author Contributions: Conceptualization, L.Z., D.Z., and Y.K.; Funding acquisition, D.Z. and Y.K.; Investigation, L.Z.; Methodology, L.Z., D.Z., S.L., S.C., and L.Z.; Project administration, Y.K. and J.X.; Resources, S.L., S.C., L.Z., and J.X.; Writing (original draft), L.Z.; Writing (review and editing), D.Z., S.S., S.W., and H.L.

Funding: This research was funded by the National Natural Science Foundation of China with grants [11674179] and [61705116] and the Program for Changjiang Scholars and Innovative Research Team in University with grant [IRT_13R29].

Conflicts of Interest: The authors declare no conflict of interest.

References

1. Wang, C.; Zhang, M.; Stern, B.; Lipson, M.; Lončar, M. Nanophotonic lithium niobate electro-optic modulators. *Opt. Express* **2018**, *26*, 1547–1555. [[CrossRef](#)] [[PubMed](#)]
2. Dhar, L.; Curtis, K.; Fäcke, T. Holographic data storage: coming of age. *Nat. Photonics* **2008**, *2*, 403–405. [[CrossRef](#)]
3. Wang, Y.; Zhou, S.X.; He, D.H.; Hu, Y.; Chen, H.X.; Liang, W.G.; Yu, J.H.; Guan, H.Y.; Luo, Y.H.; Zhang, J.; et al. Electro-optic beam deflection based on a lithium niobate waveguide with microstructured serrated electrodes. *Opt. Lett.* **2016**, *41*, 4739–4742. [[CrossRef](#)] [[PubMed](#)]

4. Bazzan, M.; Sada, C. Optical waveguides in lithium niobate: Recent developments and applications. *Appl. Phys. Rev.* **2015**, *2*, 040603. [[CrossRef](#)]
5. Jiang, H.W.; Luo, R.; Liang, H.X.; Chen, X.F.; Chen, Y.P.; Lin, Q. Fast response of photorefraction in lithium niobate microresonators. *Opt. Lett.* **2017**, *42*, 3267–3270. [[CrossRef](#)] [[PubMed](#)]
6. Tu, D.; Xu, C.N.; Yoshida, A.; Fujihala, M.; Hirotsu, J.; Zheng, X.G. LiNbO₃:Pr³⁺: A multipiezo material with simultaneous piezoelectricity and sensitive piezoluminescence. *Adv. Mater.* **2017**, *29*, 1606914. [[CrossRef](#)] [[PubMed](#)]
7. Gopalan, K.K.; Janner, D.; Nanot, S.; Parret, R.; Lundeberg, M.B.; Koppens, F.H.L.; Pruneri, V. Mid-infrared pyroresistive graphene detector on LiNbO₃. *Adv. Opt. Mater.* **2017**, *5*, 1600723. [[CrossRef](#)]
8. Lengyel, K.; Péter, Á.; Kovács, L.; Corradi, G.; Pálfalvi, L.; Hebling, J.; Unferdorben, M.; Dravecz, G.; Hajdara, I.; Szaller, Z.; et al. Growth, defect structure, and THz application of stoichiometric lithium niobate. *Appl. Phys. Rev.* **2015**, *2*, 040601. [[CrossRef](#)]
9. Hesselink, L.; Orlov, S.S.; Liu, A.; Akella, A.; Lande, D. Neurgaonkar, R.R. Photorefractive materials for nonvolatile volume holographic data storage. *Science* **1998**, *282*, 1089–1094. [[CrossRef](#)] [[PubMed](#)]
10. Schmidt, W.G.; Albrecht, M.; Wippermann, S.; Blankenburg, S.; Rauls, E.; Fuchs, F.; Rödl, C.; Furthmüller, J.; Hermann, A. LiNbO₃ ground- and excited-state properties from first-principles calculations. *Phys. Rev. B* **2008**, *77*, 035106. [[CrossRef](#)]
11. Bernert, C.; Hoppe, R.; Wittwer, F.; Woike, T.; Schroer, C.G. Ptychographic analysis of the photorefractive effect in LiNbO₃:Fe. *Opt. Express* **2017**, *25*, 31640–31650. [[CrossRef](#)] [[PubMed](#)]
12. Yang, Y.P.; Buse, K.; Psaltis, D. Photorefractive recording in LiNbO₃:Mn. *Opt. Lett.* **2002**, *27*, 158–160. [[CrossRef](#)] [[PubMed](#)]
13. Ren, L.Y.; Liu, L.R.; Liu, D.A.; Zu, J.F.; Luan, Z. Optimal switching from recording to fixing for high diffraction from a LiNbO₃:Ce:Cu photorefractive nonvolatile hologram. *Opt. Lett.* **2004**, *29*, 186–188. [[CrossRef](#)] [[PubMed](#)]
14. Volk, T.R.; Rubina, N.M.; Pryalkin, V.I.; Krasnikov, V.V.; Volkov, V.V. Optical and Nonlinear Optical Investigations in LiNbO₃: Mg and LiNbO₃:Zn. *Ferroelectrics* **1990**, *109*, 345–350. [[CrossRef](#)]
15. Fang, S.F.; Han, Z.X.; Qiao, Y.J.; Liu, Y.Y.; Jia, Q. Defect structure characteristics in near-stoichiometric In:LiNbO₃ single crystals grown by K₂O-flux method. *Cryst. Res. Technol.* **2009**, *44*, 1211–1214. [[CrossRef](#)]
16. Minzioni, P.; Cristiani, I.; Yu, J.; Parravicini, J.; Kokanyan, E.P.; Degiorgio, V. Linear and nonlinear optical properties of Hafnium-doped lithium-niobate crystals. *Opt. Express* **2007**, *15*, 14171–14176. [[CrossRef](#)] [[PubMed](#)]
17. Tian, T.; Kong, Y.F.; Liu, S.G.; Li, W.; Wu, L.; Chen, S.L.; Xu, J.J. Photorefractive of molybdenum-doped lithium niobate crystals. *Opt. Lett.* **2012**, *37*, 2679–2681. [[CrossRef](#)] [[PubMed](#)]
18. Shi, H.X.; Ren, C.Y. Investigation on photorefractive properties of Hf: Fe: LiNbO₃ crystals. *Opt. Int. J. Light Electron Opt.* **2013**, *124*, 3170–3172. [[CrossRef](#)]
19. Fujimura, R.; Shimura, T.; Kuroda, K. Two-color nonvolatile holographic recording and light-induced absorption in Ru and Fe codoped LiNbO crystals. *Opt. Mater.* **2009**, *31*, 1194–1199. [[CrossRef](#)]
20. Fan, Y.X.; Xu, C.; Wang, Y.J.; Xia, S.X.; Guan, C.X.; Cao, L.C. Influence of ZnO codoping on growth and holographic properties of Ru/Fe double-doped LiNbO₃ single crystals. *J. Cryst. Growth* **2011**, *318*, 657–660. [[CrossRef](#)]
21. Tian, T.; Kong, Y.F.; Liu, S.G.; Li, W.; Chen, S.L.; Rupp, R.; Xu, J.J. Fast UV-Vis photorefractive response of Zr and Mg codoped LiNbO₃:Mo. *Opt. Express* **2013**, *21*, 10460. [[CrossRef](#)] [[PubMed](#)]
22. Danai, M.M. Czochralski method. In *Dictionary of Gems and Gemology*, 3rd ed.; Springer: Berlin/Heidelberg, Germany, 2009; p. 289. ISBN 978-3-540-72795-8.
23. Yan, W.B.; Shi, L.H.; Chen, H.J.; Shen, X.N.; Kong, Y.F. Investigations of the OH[−] absorption bands in congruent and near-stoichiometric LiNbO₃: Hf crystals. *EPL* **2010**, *91*, 36002. [[CrossRef](#)]
24. Smith, R.G.; Fraser, D.B.; Denton, R.T.; Rich, T.C. Correlation of reduction in optically induced refractive-index inhomogeneity with OH content in LiTaO₃ and LiNbO₃. *J. Appl. Phys.* **1968**, *39*, 4600–4602. [[CrossRef](#)]
25. Kong, Y.F.; Zhang, W.L.; Chen, X.J.; Xu, J.J.; Zhang, G.Y. OH[−] absorption spectra of pure lithium niobate crystals. *J. Phys. Condens. Mater.* **1999**, *11*, 2139. [[CrossRef](#)]
26. Li, S.Q.; Liu, S.G.; Kong, Y.F.; Deng, D.L.; Gao, G.Y.; Li, Y.B.; Gao, H.C.; Ling, Z.; Hang, Z.H.; Chen, S.L.; et al. The optical damage resistance and absorption spectra of LiNbO₃:Hf crystals. *J. Phys. Condens. Matter* **2006**, *18*, 3527. [[CrossRef](#)]

27. Kovács, L.; Szalay, V.; Capelletti, R. Stoichiometry dependence of the OH⁻ absorption band in LiNbO₃ crystals. *Solid State Commun.* **2015**, *52*, 1029–1031. [[CrossRef](#)]
28. Kovács, L.; Szaller, Z.; Lengyel, K.; Corradi, G. Hydroxyl ions in stoichiometric LiNbO₃, crystals doped with optical damage resistant ions. *Opt. Mater.* **2014**, *37*, 55–58. [[CrossRef](#)]



© 2018 by the authors. Licensee MDPI, Basel, Switzerland. This article is an open access article distributed under the terms and conditions of the Creative Commons Attribution (CC BY) license (<http://creativecommons.org/licenses/by/4.0/>).